A STUDY OF THERMAL REGIME IN THE HIGH-POWER LED ARRAYS

A.V. Aladov[1], I.V. Belov[2], V.P. Valyukhov[3], A.L. Zakgeim[1], A.E. Chernyakov[1]

[1] Submicron Heterostructures for Microelectronics, Research & Engineering Center of RAS, St. Petersburg, Russian Federation;

[2] Jönköping University, School of Engineering, Jönköping, Sweden;

[3] Peter the Great St. Petersburg Polytechnic University, St. Petersburg, Russian Federation

Thermal resistance and temperature distribution for high-power AlGaInN LED chip-on-board arrays were measured by different methods and tools. The p—n junction temperature was determined through measuring a temperature-dependent forward voltage drop on the p—n junction, at a low measuring current after applying a high heating current. Furthermore, the infrared thermal imaging technique was employed to obtain the temperature map for the test object. A steady-state 3D computational model of the experimental setup was created including temperature-dependent power dissipation in the LED chips. Simulations of the heat transfer in the LED array were performed to further investigate temperature gradients observed in the measurements. Simulations revealed possible thermal deformation of the assembly as the reason for the hot spot formation. The bending of the assembly was confirmed by surface curvature measurements.

Key words: LED, LED matrix, thermal resistance, infrared thermography, thermal interface, CFD model

Citation: A.V. Aladov, I.V. Belov, V.P. Valyukhov, A.L. Zakgeim, A.E. Chernyakov, A study of thermal regime in the high-power LED arrays, St. Petersburg Polytechnical State University Journal. Physics and Mathematics. 11 (3) (2018) 28—37. DOI: 10.18721/JPM.11304

Introduction

Recent research into development and applications of light-emitting diode (LED) sources for general lighting has involved increasing operating currents and packing densities of light-emitting chips in the arrays to provide ever higher output powers [1, 2]. Increased power and complex construction of LED sources entail paying more attention to thermal processes both in individual LEDs and in the array as a whole. It is insufficient to estimate the total thermal resistance in this case: the temperature field distribution over the area (thermal mapping) has to be analyzed.

Since temperature considerably affects the internal quantum efficiency (IQE), its distribution becomes a factor determining the overall output characteristics of LED arrays (optical power and efficiency). Accordingly, exploring the non-uniform temperature distribution over the array as a function of current is particularly important for modern high-power LED arrays.

The goal of this study has been detailed analysis of thermal resistance and temperature distribution in high-power white LED arrays.

Experimental procedure

We have experimentally studied the thermal processes in LED arrays manufactured by the chip-on-board technology [3] using high-power face-up AlInGaN LED chips [4]. Finding the exact temperature gradients on the surface of a LED array, associated with non-uniform heat generation and dissipation from each chip in this array, is of particular

interest in this context. To this end, we have carried out detailed simulation of thermal and current distribution in a real LED array, and determined the temperature of emitting chips located at different points of the array by direct and indirect experimental methods.

The direct method for estimating the temperature of LED chips is based on high-resolution infrared thermography using a SVIT IR thermal imaging camera [5, 6]. Thermal resistance was measured by relaxation of the temperature-dependent parameter (forward voltage) with a T3Ster thermal transient tester [7, 8].

This section describes the experimental samples and the experimental methods used for estimating the thermal characteristics, including measurements of thermal resistances, IR mapping, and measuring the thermal deformation of the LED array in operating mode.

Experimental samples. We have studied high-power arrays based on commercial ES-CABLV45P chips by EpiStar. The emitting chips have a face-up configuration [9], where an epitaxial AlInGaN heterostructure is stored on a sapphire substrate with low thermal conductivity (≈ 0.34 W/cm·K). Both contacts are located on the face, and the light is transmitted through a semitransparent *p*-contact. The emitting chips have a complex "branching" topology of the electrodes to achieve a uniform current distribution at an operating current of 400 mA [10]. LED chips 1140×1140 μm in size and 150 μm thick were mounted onto an aluminum-core printed circuit board (MCPCB) using the chip-on-board (COB) technology. The LED array was an assembly consisting of 100 chips 45×45×1.0 mm in size with a total input power of up to 100 W, which corresponds to a current of 350 mA passing through a single chip.

The LED array comprised 10 parallel-connected LED rows, each including 10 series-connected chips. The total area of the LED assembly was 20 Ч 20 mm. The chips were protected with a silicone gel containing luminophore.

The aluminum plate with the LED array was screwed to a heatsink. The diagonal distance between the heads of the screws fixing the board to the heatsink was 44 mm. The appearance of the LED array and a cross-sectional view of the structure are shown in Fig. 1.

Measurement of thermal resistances. Thermal resistances were determined using the electric analogy where heat flow is considered instead of electric current and temperature instead of voltage. Heat is transferred from the active region to the chip substrate, then to the aluminum plate through the glue, then through the thermal paste to the heatsink, which comprise elements of an equivalent thermal circuit: chip (R_{chip}), glue (R_{glue}), aluminum plate ($R_{Al\ plate}$). The Cauer model suggests that such a chain consists of a set of thermal resistors connected to a common bus through thermal capacities. The thermal capacities of different layers of the LED assembly affect only the transient characteristics, i.e., either the heating or cooling rates of the device when the current is switched on/off.

To determine the thermal resistance by the temperature-dependent parameter (the forward voltage drop time), the array was initially switched to a low test current of 50 mA so that

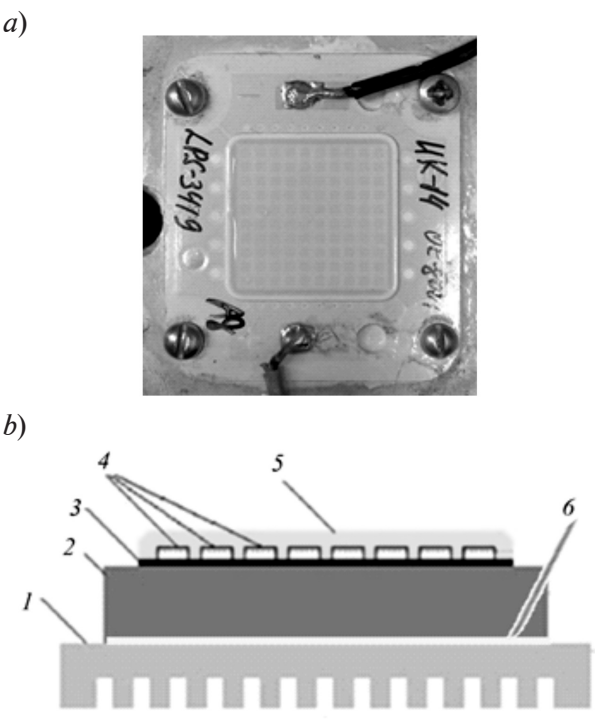

Fig. 1. LED array: appearance from above (*a*) and schematic cross-sectional view (*b*)
heatsink *1*, aluminum board *2*, glue *3*, LED chips *4*, silicone gel *5*, thermal paste *6*

the device would not self-heat, and the temperature of the p—n-junction was set by an external heater in the range of 20 – 100 °C with an accuracy of 0.5°C. Forward voltage was recorded as a function of temperature. A calibration curve for forward voltage versus temperature was obtained this way; the curve is close to a linear dependence with a coefficient of −13 mV/K. This value was subsequently used to determine the temperature of the p—n-junction in real operating mode.

The forward voltage drop (a transient characteristic) was studied with rapid switching from a low test current to a high operating one. The device was gradually heated from that moment, with heat transferred from the active region through the chip and the PC board to the heatsink and the ambient environment. The temperature evolution of the p—n junction under heating was measured by the changes in the forward voltage at the moment when short test current pulses, "cutting" the direct heating operating current, were supplied at a specific frequency. Subsequent mathematical analysis of the transient voltage characteristic in the p—n junction using the structure function approach [11] allowed to calculate the components $R_{th,I}$ and $C_{th,i}$ of the equivalent thermal circuit, the total thermal resistance ΣR_{th} and the total heat capacity ΣC_{th}. The continuous cumulative structure function was approximated by a step function, which was a direct representation of Cauer's thermal impedance model. The methods of transient characteristics and the mathematical tools involved are discussed in more detail in [12] and the references cited therein.

The T3Ster was originally intended for electronic devices, and its data processing is based on the premise that electrical power supplied to the device is completely converted to heat. However, a significant fraction of the supplied electric power in modern high-performance LEDs is converted to light and, therefore, does not contribute to heating the device. To account for this, output optical power P_{opt} was measured using the OL 770-LED High Speed LED Test and Measurement system with an integrating sphere [13]. The wall-plug efficiency for the given array amounted to 15 – 20% (depending on the input current). The corresponding part of the input power carried away by radiation was taken into account in calculations of thermal resistance.

IR thermal imaging. Temperature of the LED array surface was measured using a SVIT IR thermal imaging camera with a sensitivity range of 2.5 – 3.0 μm [10]. Measuring the temperature directly with a thermal imager allows obtaining the temperature area distribution (so-called thermal mapping).

The main methodological issues encountered in thermal mapping of AlInGaN-based structures are, firstly, that the sapphire substrate and epitaxial layers are transparent for IR wavelengths, and, secondly, that the emissivities of the materials used in LEDs (semiconductor layers, metal contacts, reflective coatings, mounting elements, etc.) are largely different [14]. For this reason, preliminary calibration is required to extract the correct temperature distributions from the IR images. This calibration was carried out, with the temperature maintained by an external heater in the range from 20 to 100 °C, by recording the IR radiation from the LED array at zero current. Using this approach, we were able to measure

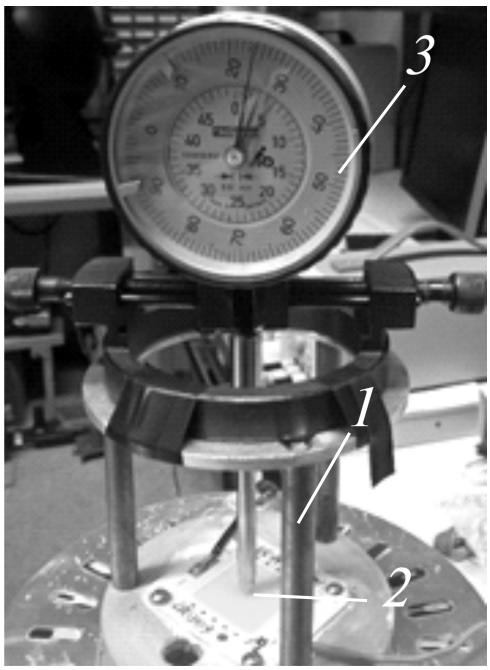

Fig. 2. Photograph of the spherometer used to measure the curvature radius of the LED array:
metal tripod 1, pointed tip 2, gauge 3

the temperature with an accuracy up to 2 K.

Measurements of the surface curvature. We used a spherometer with a dial gauge (SЬSS MicroTec, Germany) to estimate the thermal deformation of the LED array during operation, measuring the elevation of the center of the LED array in operating mode (with a current of 3.5 A) compared to the position of this center at zero current.

The spherometer consists of a metal tripod with three fixed legs of the same length (Fig. 2 [15]), a pointed tip passing along the center of the frame parallel to the legs and a standard dial gauge with a 0.01 mm graduation, showing the elevation of the tip above or below the surface on which the legs of the spherometer are resting. The position of the tip can be read with an accuracy of 5 μm.

A stationary hydrodynamic model (Computational Fluid Dynamics, CFD) was used for a flat LED array at the first stage of simulating the heat dissipation; possible deformation of the LED array (curvature of the heatsink surface) was taken into account at the next stage.

A stationary CFD model describing the thermal processes in the experimental samples was created in Flotherm 10.1 by Mentor Graphics (Fig. 3 [16]). The goal of the simulation was to reproduce the results obtained in the experiment and to study the causes of temperature gradients between the center and the periphery of the LED array. A large cylindrical aluminum heatsink was approximated by an aluminum block, and the effect of cooling fins by a high heat transfer coefficient (10,000 W/(m^2·K)) applied to the walls of the aluminum block.

The adhesive (glue) layer used to mount the chip and the thermal paste layer (15 μm thick) between the plate and the heatsink were simulated as thermal resistances at the respective interfaces. The protective silicone gel layer had a thickness of 300 μm. The thermal resistance of the glue, equal to 2.6 K/W for each chip, was obtained from the total structure function corresponding to a heating current of 1 A. This current value provided the most uniform heating of the LED array. The thermophysical properties of the materials are given in Table.

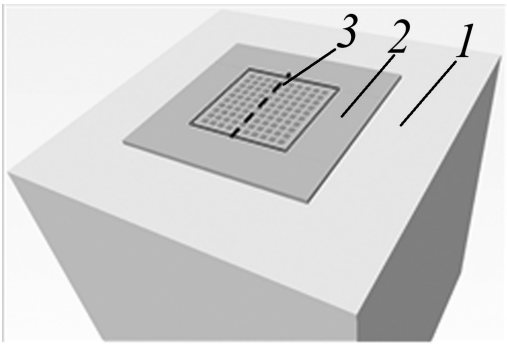

Fig. 3. CFD model of the experimental setup
aluminum block 1; LED array 2 coated with silicone gel; central part of the array (indicated by the dashed line)

Constant pressure was imposed at the boundaries of the computational domain. The ambient temperature was 20°C. The model also included thermal radiation. An algebraic turbulence model was used for the simulation. Grid-independent results were obtained by simulating a model with different cell densities. The computational domain contained 1.8 million cells with local grids for LED chip, silicone gel and aluminum board. The dependence of the power emitted by LEDs on temperature at a fixed voltage applied to the array (Fig. 4) was obtained by measurements of a single chip and included optical cooling.

Table

Thermophysical properties of the simulated system [16 −18]

System component (material)	Thermal conductivity, W/(m·K)	Density, kg/m^3
LED chip (sapphire)	36.0	3980.0
Board and heatsink (aluminum)	201.0	2710.0
Protective gel (silicone)	1.0	1000.0
Thermal paste	0.67	–

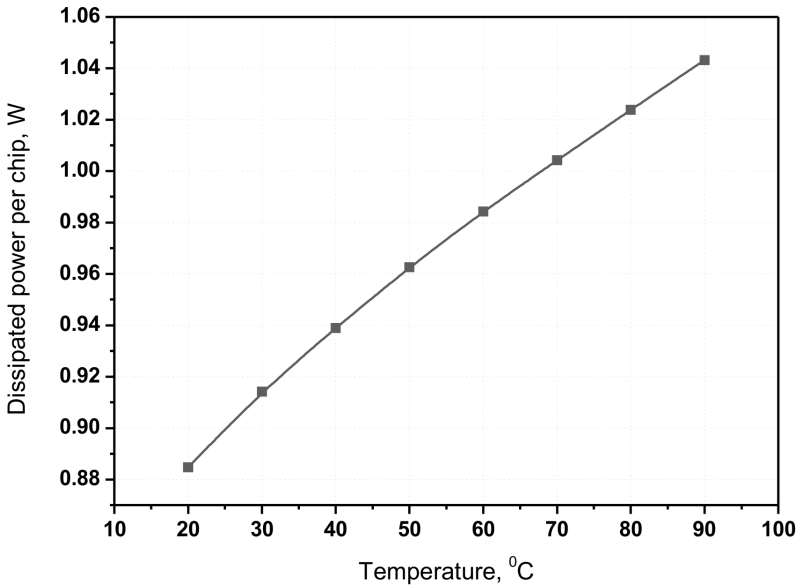

Fig. 4. Dissipated power as a function of temperature for a single LED chip

Results and discussion

The results of the measured thermal resistances for the LED array are given in Fig. 5 as cumulative structure functions. The values of thermal resistance R_{th} are plotted along the horizontal axis, and the values of specific heat C_{th} from the heat source to the ambient (shown on a logarithmic scale) are plotted along the vertical axis.

The value of the total thermal resistance

$$\Sigma R_{th} = R_{chip} + R_{glue} + R_{Al\ plate} \qquad (1)$$

was obtained for three currents: 1.0, 3.5 and 4.0 A. Evidently, quantity (1) increases from 0.3 to 0.5 K/W (by about 1.7 times) with increasing current. The inflection points on the curves indicate the thermal resistances measured along the thermal circuit. The increase in thermal resistance with increasing current can be explained by its redistribution in favor of the central arrays compared to the peripheral ones, and thus reduced sizes of the heat generation and, accordingly, the heat dissipation regions. However, the difference in the currents turned out to be insignificant (within 4 %), so heat generation can be considered nearly homogeneous in the entire LED array. This means that the increase in thermal resistance with increasing current is associated with the changes in heat dissipation rather than in in heat generation.

Heat transfer from the center of the array to the ambient is worse than at the periphery of the plate. This was confirmed by direct measurement of heat distribution with an IR thermal imaging camera. The observed temperature distribution along the central axis of the array is shown in Fig. 6. A noticeable temperature difference up to 13 K is observed between the central and peripheral chips of the array.

First simulations revealed a 3 – 4 K maximum temperature variation between the center and the periphery of the LED array. The CFD model initially implied that the thermal resistance between the aluminum plate and the heatsink did not vary at different points, that is, the thermal paste layer between the aluminum plate and the radiator was assumed to be homogeneous.

Upon analysis of the computational data and closer inspection of the LED array samples, we have hypothesized that the temperature variation (up to 13 K) between the central and

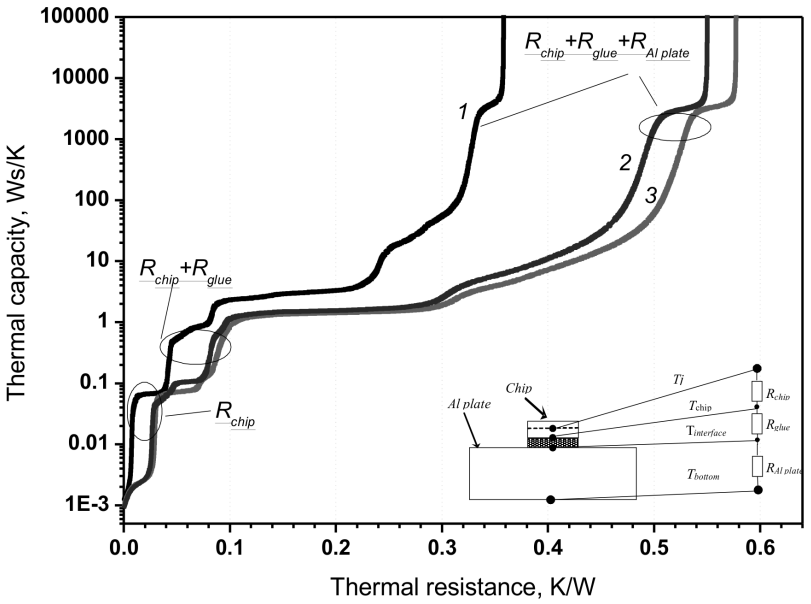

Fig. 5. Cumulative structural functions (thermal capacity versus thermal resistance) for the LED array with different currents, A: 1.0 (1) 3.5 (2) and 4.0 (3). The inset shows a simplified diagram of the thermal circuit

peripheral chips could be caused by bending of the aluminum plate. Bending also occurs due to intense heating of LED chips under rigid mechanical constraints imposed by screws in the corners of the plate

Thermal deformation of the LED array was measured by a spherometer at two points: at the center of the aluminum plate and next to one of the screws. Vertical shift in operating mode was 80 μm at the center of the LED array, and almost did not change near the screw. Therefore, the experiment confirmed

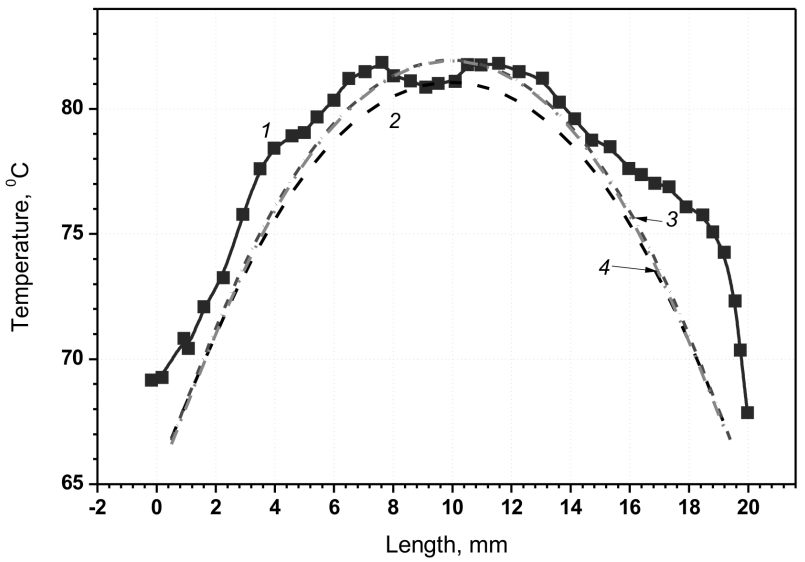

Fig. 6. Experimental (symbols 1) and calculated (lines 2 – 4) temperature distributions along the central axes of the LED arrays

that overheating at the center of the LED array is due to thermal deformation of the aluminum plate, leading to deterioration of the thermal contact between the aluminum plate and the heatsink.

The deterioration in thermal resistance at the interface between the aluminum plate and the heatsink was taken into account in the model by partitioning the thermal resistances between the heatsink and the aluminum plate into zones. Fig. 7 shows examples of the aluminum board partitioned into 4 and 6 zones of thermal resistances. The partitioning was based on the assumption that the variation (growth) in thermal resistance near the edges of the plate should be less compared to the center due to the plate's bending. The thermal resistance values assigned to individual zones were obtained by calibrating the simulated temperatures with respect to the measurements obtained in the central part of the LED array (the surface temperature of silicone is higher than 80 – 82 °C for the central chips and 65 – 68 °C for the periphery, see Fig. 6). The results of partition into thermal zones were additionally compared with the results for the resistances of a homogeneous thermal paste layer (without partitioning). Using thermal resistance zones in the model led to achieving good agreement with the experimental data in the measured temperature range. The thermal resistance values for the thermal zones are shown in Fig. 8, and the results of simulation and comparison between the measured data and the simulated temperatures are shown in Fig. 6. We have tested the results of partitions into a different number of zones. It can be seen from the data in Fig. 6 that no considerable variation could be observed in the results obtained by increasing the number of thermal resistance zones to six, compared with a coarser partition.

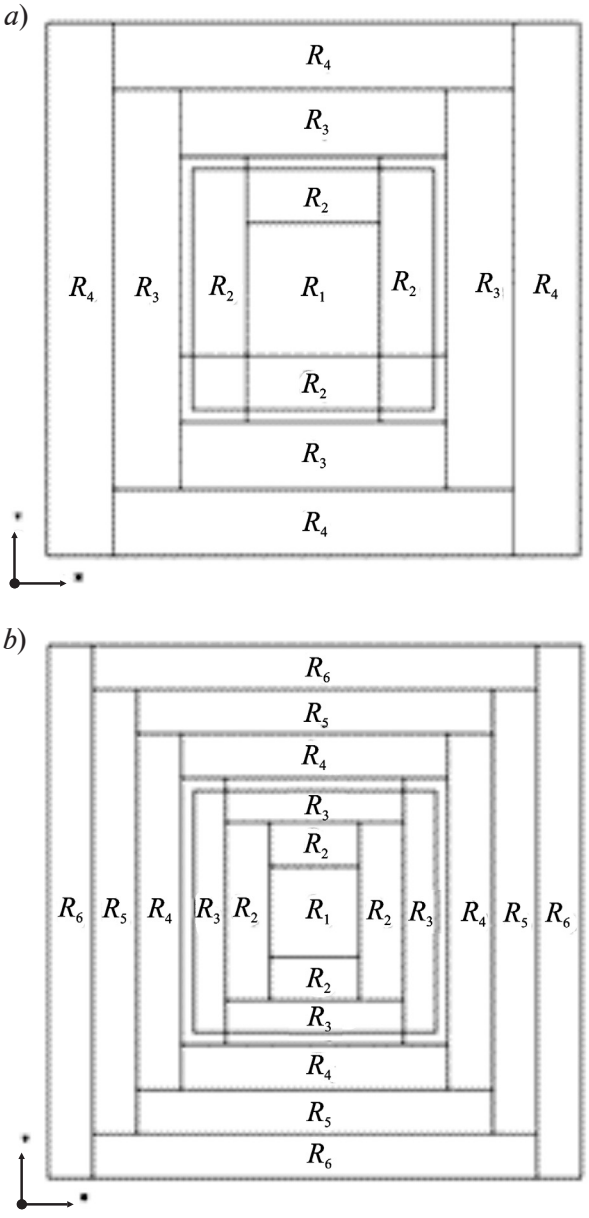

Fig. 7. Selected partitions of the aluminum board model into 4 (a) and 6 (b) zones of thermal resistance (Ri is the resistance of an ith zone)

The good agreement between the simulated and experimental temperatures obtained by partitioning the thermal resistances is shown in Fig. 6.

It is evident from the results of multizonal partitioning that thermal resistance significantly deteriorates starting from the zone next to the edge of the aluminum plate (i.e., R_3 and R_5). This is consistent with the fact that no continuous thermal paste layer could be found under the bent part of the aluminum board. Since the total measured bending height was 80 μm and the maximum thickness of the thermal paste layer was 15 μm, the area filled with thermal paste could only be located below the zone corresponding to the thermal resistance R_4 (for partition into four zones) or

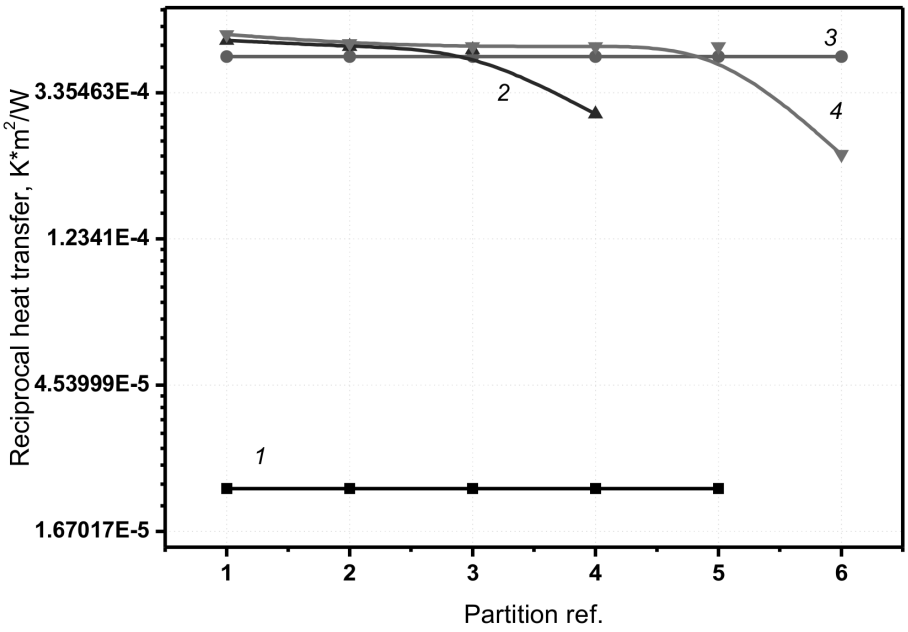

Fig. 8. Inverse thermal conductivity coefficients corresponding to different partition zones with respect to the resistance of the homogeneous thermal paste layer:
homogeneous thermal paste layer 1, four partition zones 2, without partition into zones 3, six partition zones 4

R_6 (for partition into six zones). The effective thermal resistance of these zones, 0.1 K/W, determined by calibrating the model, was approximately 10 times worse than the thermal resistance of a homogeneous thermal paste layer of 0.011 K/W under a non-deformed aluminum plate. A possible explanation for such a high value is that the aluminum plate is deformed along the edges under heating. It is also clear from the simulation results and temperature measurements that the effect of thermal deformation of the aluminum plate on the temperature distribution profile of the LED array can be represented by one effective thermal resistance, as shown in Fig. 6 and 8, i.e., without partitioning. Using this alternative is not substantiated from a physical standpoint, but leads to satisfactory agreement between the simulated and measured temperature.

The temperature distribution over the area of the LED array is shown in Fig. 9. The method of partitioning the thermal resistances allows to predict the formation of local hot spots on the array surface, and thus reproduces the effect of the measured thermal deformation of the aluminum plate.

Conclusion

We have carried out experiments and computer simulation to study the thermal properties of high-power white AlInGaN LED arrays based on emitting face-up chips mounted on an aluminum MCPCB board using the chip-on-board technology. Experimental studies

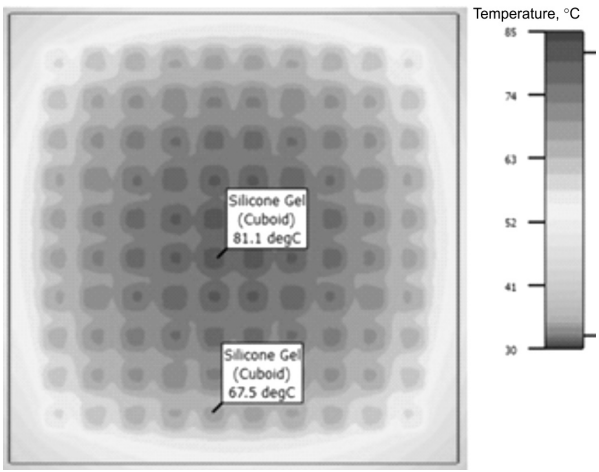

Fig. 9. Calculated temperature map for the surface of the LED array (with thermal deformation taken into account)

involved both indirect methods for determining thermal parameters from the transient temperature-dependent characteristics and a direct method for determining the temperature via IR thermal imaging.

We have established that the total thermal resistance of the LED array increased by 1.7 times as the operating current increased from 1 to 4 A, due to significant deterioration in heat removal from the chips located at the center of the array compared to those located on the periphery. This is a consequence of deformation caused by linear thermal expansion: more specifically, the central part bends as the aluminum board is fixed by the corners with screws, the gap between this board and the heatsink widens and the thermal contact deteriorates. The latter is confirmed both by the temperature distribution obtained from IR temperature mapping, and by direct measurement of the curvature of the LED array's surface in operating mode.

Mathematical and experimental simulation played a key role in understanding the observed phenomenon of thermal deformation. A small change in surface temperature, obtained as a result of CFD simulation with a homogeneous layer of thermal paste, allowed us to suggest thermal deformation of the LED array to be the reason for the actually measured temperature gradient. The simulation results were then confirmed by direct measurement of a significant bending height (up to 80 μm) of the aluminum board in operating mode.

Additionally, we have proposed a method for breaking the thermal resistance into zones, giving an example of CFD simulation of experimental samples which is in good agreement with thermal imaging results. The difference in temperature between the central and peripheral chips can reach 13 K at an input power of 100 W. Overheating of the central chips reduces the service life of the LED array. This should be taken into account when estimating the thermal resistances obtained by forward voltage drop.

Finally, the given combination of experimental methods and simulation techniques should be of help to electronics developers, facilitating analysis and solution of reliability problems caused by local hot spots evolving in the LED array as a result of thermomechanical deformation of the array's components during operation.

Measurements of LED characteristics were carried out at the Collective Use Center "Hardware components of radiophotonics and nanoelectronics: technology, diagnostics, metrology", St. Petersburg, Russian Federation.

REFERENCES

[1] **Zh. Ping, Z. Jianhua, C. Xianping C., et al.,** An experimental investigation of a 100-W high-power light-emitting diode array using vapor chamber-based plate, Advances in Mechanical Engineering. 7 (11) (2015) 1–7. https//doi.org/10.1177/1687814015620074.

[2] **F. Jiajie, X. Chaoyi, Q. Cheng, et al.,** Luminescence mechanism analysis on high power tunable color temperature Chip-on-Board white LED modules, Proc. of the 18th International Conference on Thermal, Mechanical and Multi-Physics Simulation and Experiments in Microelectronics and Microsystems (EuroSimE), 3–5 April 2017, Dresden, Germany (2017) 1–6.

[3] **H.L. John,** Chip on board, Technology for multichip modules, Springer, New York, 1994.

[4] **S.G. Konsowski, A.R. Helland,** Electronic packaging of high speed circuitry, McGraw Hill Professional, New York, 1997.

[5] **A.G. Shusharin, V.V. Morozov, M.P. Polovinka,** Medical infrared imaging – modern features of the method, Modern problems of science and education. (4) (2011), URL: http://science-education.ru/ru/article/view?id=4726.

[6] **S.C. Ki, C.Y. Sun, K. Jae-Young, et al.,** Precise temperature mapping of GaN-based LEDs by quantitative infrared micro-thermography, Sensors. 12 (4) (2012) 4648–4660.

[7] MicReD. T3Ster, URL: https://www.mentor.com/products/mechanical/ micred/t3ster/.

[8] Thermal management for LED applications, C.J.M. Lasance, A. Poppe (Eds), Springer, New York, 2014.

[9] ES-CABLV45P data sheet, 2017, URL: http://www.epistar.com. tw/upfiles/files_/ES-CABLV45P.pdf

[10] **A.V. Aladov, K.A. Bulashevich, A.E. Chernyakov, et al.,** Thermal resistanse and nonuniform distribution of electroluminescence and temperature in high-power AlGaInN light-emitting diodes, St. Petersburg Polytechnical University Journal: Physics and Mathematics. (2 (218)) (2015) 151–158.

[11] **D. Schweitzer, H. Pape, L. Chen, et**

al., Transient dual interface measurement – A new JEDEC standard for the measurement of the junction-to-case thermal resistance, Proc. of the 27th Annual IEEE Semiconductor Thermal Measurement and Management Symposium (SEMI-THERM'11), 20–24 March, 2011, San Jose, USA. (2011) 222–229.

[12] **V.I. Smirnov, V.A. Sergeev, A.A. Gavrikov,** Apparatus for measurement of thermal impedance of high-power light-emitting diodes and LED assemblies, IEEE Transactions on Electron Devices. 63 (6) (2016) 2431–2435.

[13] **A.L. Zakgeim, G.L. Kuryshev, M.N. Mizerov, et al.,** A study of thermal processes in highpower InGaN/GaN FlipC-hip LEDs by IR thermal imaging microscopy, Semiconductors. 44 (3) (2010) 373–379.

[14] **R.H. Hopper, I. Haneef, S.Z. Ali, et al.,** Use of carbon micro-particles for improved infrared temperature measurement of CMOS MEMS devices, Measurement Science and Technology. 21 (4) (2010) 1–6.

[15] **R.P. Shukla, D. Udupa,** Measurement of radius of curvature of cylindrical surfaces, Journal of Optics (India). 30 (3) (2001) 131–142.

[16] Mentor Graphics Corporation. Flotherm v.10.1 User Manual (2014).

[17] Silicone Gel, 2017, URL: https://www.acc-silicones.com.

[18] Organo-silicon heat-conducting paste, Specifications, 2017, URL: http://pripoi.ru.

[19] **A.L. Zakgeim, A.E. Chernyakov,** A measuring system for obtaining spectroradiometric, photocolorimetric, and thermal characteristics of semiconductor radiators, Light and Engineering. 21 (4) (2013) 64–70.

Received 25.06.2018, accepted 09.07.2018.

THE AUTHORS

ALADOV Andrey V.
Submicron Heterostructures for Microelectronics Research and Engineering Center of the RAS
26 Politechnicheskaya St., St. Petersburg, 195251, Russian Federation
aaladov@mail.ioffe.ru

BELOV Ilia V.
Jönköping University, School of Engineering
5 Gjuterigatan St., Jönköping, Sweden
ilia.belov@ju.se.ru

VALYUKHOV Vladimir P.
Peter the Great St. Petersburg Polytechnic University
29 Politechnicheskaya St., St. Petersburg, 195251, Russian Federation
Valyukhov@yandex.ru

ZAKGEIM Alexader L.
Submicron Heterostructures for Microelectronics Research and Engineering Center of the RAS
26 Politekhnicheskaya St., St. Petersburg, 194021, Russian Federation
zakgeim@mail.ioffe.ru

CHERNYAKOV Anton E.
Submicron Heterostructures for Microelectronics Research and Engineering Center of the RAS
26 Politekhnicheskaya St., St. Petersburg, 194021, Russian Federation
chernyakov.anton@yandex.ru